J. Chem. Sci. Vol. 127, No. 12, December 2015, pp. 2119–2135.
DOI 10.1007/s12039-015-0987-7

Pyrolysis of 3-carene: Experiment, Theory and Modeling

N SHARATH[a], H K CHAKRAVARTY[b,#], K P J REDDY[a], P K BARHAI[c] and E ARUNAN[b,*]

[a]Department of Aerospace Engineering Indian Institute of Science, Bangalore, India
[b]Department of Inorganic and Physical chemistry, Indian Institute of Science, Bangalore, India
[c]Department of Applied Physics, Birla Institute of Technology, Mesra, Ranchi, India
[#]Current Address: Max Planck Institute for Chemistry, Mainz, Germany
e-mail: arunan@ipc.iisc.ernet.in

MS received 7 July 2015; revised 28 August 2015; accepted 31 August 2015

Abstract. Thermal decomposition studies of 3-carene, a bio-fuel, have been carried out behind the reflected shock wave in a single pulse shock tube for temperature ranging from 920 K to 1220 K. The observed products in thermal decomposition of 3-carene are acetylene, allene, butadiene, isoprene, cyclopentadiene, hexatriene, benzene, toluene and p-xylene. The overall rate constant for 3-carene decomposition was found to be

$$k/s^{-1} = 10^{(9.95\pm0.54)}\ \exp(-40.88 \pm 2.71\,\text{kcal mol}^{-1}/RT).$$

Ab-initio theoretical calculations were carried out to find the minimum energy pathway that could explain the formation of the observed products in the thermal decomposition experiments. These calculations were carried out at B3LYP/6-311+G(d,p) and G3 level of theories. A kinetic mechanism explaining the observed products in the thermal decomposition experiments has been derived. It is concluded that the linear hydrocarbons are the primary products in the pyrolysis of 3-carene.

Keywords. Shock Tube; Monoterpene; Thermal Decomposition; Isoprene.

1. Introduction

Understanding the chemistry of hydrocarbons in the combustion and soot formation process is one of the growing research topics. Molecules like cyclohexane were previously used as a model molecule to derive and extend the pyrolysis and combustion mechanism for higher hydrocarbons.[1] It is well known that the ignition of fuels will be preceded by its pyrolysis. The radicals formed from the decomposition will either react with oxygen or with other molecules/radicals to give products. Thus, the decomposition studies of hydrocarbons, which have the characteristics of a fuel, could be useful in understanding the combustion and soot formation process.

Kinetics of kerosene based molecules such as JP-10, which is used as a rocket fuel has been well studied.[2–5] 3-carene, a bi-cyclic monoterpene, the molecular structure of which is shown in figure 1, has the same molecular formula as that of JP-10, $C_{10}H_{16}$. Initial extraction of 3-carene was carried out by Simonsen from a grass, *Pinuslongifolia*, obtained from Himalayas and the hills ranging from Kashmir to Assam.[6–8] Recently, Siavash *et al.*[9] and Salem *et al.*[10] extracted 3-carene from other plant sources, namely, *Zeravschaniamembranacea* and *Pinusroxburghii*.

In 2009, Kulkarni *et al*. suggested a blend of 75% ethylidenenorbornene and 25% 3-carene as a promising high energy and density fuel.[11] Recently, we carried out ignition delay experiments of 3-carene/O_2/Ar mixture[12] and found that under similar conditions its ignition delay times are lower compared to that of JP-10, supporting the results from earlier work[11] that 3-carene has all important characteristics of a fuel. As mentioned above, to understand the initiation of oxidation in a fuel, knowledge of its decomposition process at higher temperature is essential. To the best of our knowledge, the only available study on thermal decomposition of 3-carene which was carried out in a heated tube and analyzed using gas liquid chromatography was focused on its isomerization process. It also gave a brief qualitative and quantitative description on the nature of products and two intermediates formed at lower temperatures.[13] The available results are not sufficient to derive a complete thermal decomposition mechanism and also, very low temperature experimental condition makes it difficult for extrapolating results to higher temperatures and pressures. Thus, the decomposition studies of 3-carene are required to understand its thermal cracking process at elevated temperatures.

*For correspondence

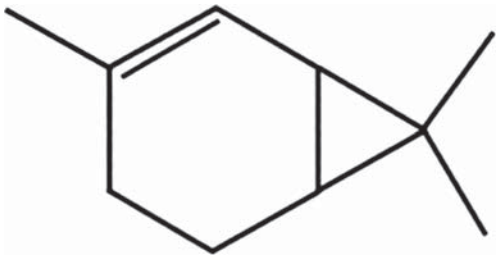

Figure 1. Two-dimensional molecular structure of 3-carene.

Also, 3-carene, being one of the abundant emitters into atmosphere from the plants, plays an important role in the atmospheric chemistry.[14–16] Somewhat surprisingly its chemistry has not been fully explored. Literature available on chemistry of 3-carene include determination of its structure[17] and its reaction with triplet oxygen[18] and nitrating agents.[19]

3-carene is one of the monoterpenes which are defined as molecules with two isoprene units. Pyrolysis studies on isoprene, C_5H_8, were carried out to understand the formation of Polycyclic Aromatic Hydrocarbons (PAH).[20,21] Recent isoprene pyrolysis studies showed that its decomposition could lead to the formation of C_1 to C_6 product molecules.[22]

This manuscript reports the first detailed study on thermal decomposition of 3-carene, a complex bicyclic hydrocarbon. Several possible decomposition pathways have been identified. The first section of the paper gives the results from thermal decomposition experiments carried out to understand the initial bond breaking process. It will be followed by discussion on theoretical results of 3-carene decomposition pathways. Results from the theoretical calculations carried out to understand the isoprene decomposition process will also be presented. A kinetic mechanism which explains the observed experimental results will be discussed as well.

2. Experimental/Computational

2.1 *Experimental Setup*

The Chemical shock tube-2 (CST-2), a single pulse shock tube was used to carry out pyrolysis experiments presented in this paper. The details of CST-2 and the experimental procedure have been described in previous papers.[12,23–26] A brief description of the experimental setup and procedure is given here. The shock tube with a driver section of length 2 m and driven section of 4.25 m and an inner diameter of 40 mm was separated using an aluminium diaphragm. The diaphragms were made from 1 mm or 0.7 mm aluminium sheets and grooved to different depths. The groove depth and initial pressure, P_1 (450-600 mm Hg), were varied to obtain the required temperatures. Before each experiment the driven section was evacuated to 10^{-4} mm Hg using an ADIXEN - ATP-400 turbo-molecular vacuum pump. Argon (99.9993% pure) and helium (99.9993% pure) were used as the driven and the driver gas, respectively. 3-carene (boiling point 168°C and density 0.857 g/mL) obtained from Sigma Aldrich was distilled before use and confirmed to be 99% pure using a GC-FID. A 2-liter sample tube was used to prepare a highly diluted 3-carene and Ar mixture. The initial 3-carene concentration was in the range of 130 ppm to 730 ppm corresponding to mole fraction of 1.3×10^{-4} to 7.3×10^{-4} in argon. The required amount of this mixture was then fed into an evacuated sample section of the shock tube.

Temperature and pressure were calculated from normal shock relation using the measured Mach number obtained from PCB sensors (Model No.113A24) placed at a distance of 0.505 m apart. A GC-FID was used in qualitative and quantitative analysis of the post-shock mixture. A HP-5, 29 m $\times$ 0.53 mm $\times$ 1.53 μm capillary column was used to separate the product molecules in the GC-FID. Nitrogen was used as a carrier gas and its flow rate was maintained at 6 mL/min. The detector, inlet and oven temperatures were maintained at 250°C, 150°C and 65°C, respectively. A separate GC-MS was used for qualitative analysis of the post shock mixture. A HP-5MS, 30 m $\times$ 0.250 mm $\times$ 0.25 μm capillary column was used to separate product molecules in GC-MS. Helium was used as a carrier gas and its flow rate was maintained at 0.5 mL/min. The oven and inlet were maintained at same temperatures as that of GC-FID. A sample cell of volume 200 mL was used to extract post-shock mixture after completion of experiment from the shock tube for further analysis. Prior to each experiment, the sample chamber and the sample cell were evacuated and blank runs were taken to ensure that there were no contaminations from the previous experiment.

2.2 *Computational Method*

Gaussian 09[27] package was used to carry out quantum chemistry calculations. All geometries were optimized at G3 and B3LYP/6-311+G(d,p) level of theories. CHEMKIN[28] has been used for numerical simulation of the reactions to explain the results. The transition state energies at G3 level of theory were manually calculated using procedure described by Curtiss *et al.*[29] The zero point energies (ZPEs) for transition states were calculated using frequencies obtained at MP2/6-31G* level of theory and hence the corresponding scaling factor of 0.9427 was used.

The procedure described in our previous paper[26] has been used to obtain thermodynamic parameters for the species used in the simulation of thermal decomposition mechanism.

3. Results and Discussion

3.1 *Experimental Observation*

The thermal decomposition experiments were carried out for temperature ranging from 920 to 1220 K. The observed dwell times in the present study were in the range of 1.35-1.76 ms. The uncertainty of obtained Mach numbers were found to be less than $\pm 1\%$. This corresponds to 20 K in terms of calculated temperature. The observed products are acetylene, allene, butadiene, isoprene, cylclopentadiene, hexatriene, benzene, toluene and p-xylene. One of the gas chromatograms of 3-carene post-shock mixture, obtained using the GC-FID, is shown in figure 2. The sensitivity of FID, the response of the FID, used in the present work to obtain the concentration of molecules from the area under of the peak (in chromatogram) are given in table S1 in Supplementary Information (SI). The sensitivity factor for each molecule was obtained by passing a known concentration of sample through GC-FID. As seen in figure 2, first three peaks are not resolved. These peaks were de-convoluted using Eq. 1 to obtain the concentrations of the product molecules corresponding to those peaks.

$$y = y_0 + \frac{A}{w\sqrt{\frac{\pi}{2}}} e^{\frac{-2(x-x_c)^2}{w^2}} \qquad (1)$$

Here, Y_0: Value of the baseline, x_c: x-ordinate of center of the peak, A: Area under the curve and w: Full width at half maximum.

High base line due to the presence of argon prevented us from identifying products below m/z of 40 using GC-MS. The products with m/z >40 were identified after matching the retention time in FID and analyzing the mass-spectrum obtained using GC-MS. The first peak in the chromatogram obtained using GC-MS (scanned for m/z >48) was found to be of butadiene and identified as the third peak in the chromatogram obtained using GC-FID. After elution of butadiene, a similar elusion pattern was observed in GC-FID and GC-MS. Hence the first two peaks in the chromatogram obtained using GC-FID were concluded to be of m/z <48. In order to identify these peaks, C_1, C_2 and C_3 compounds were passed through GC-FID to match the retention time. Acetylene was confirmed to be the first peak.

Methane, ethane and ethylene did not match the retention time of the peaks. Hence, the only peak, the second peak which was left un-assigned was concluded to be that of a C_3 molecule. Propane, propene and propyne did not match the retention time of the second peak. Hence, the peak was assigned to allene. Theoretical calculations and kinetic simulation also support the formation of allene as the C_3 product. This was inferred after considering the barriers involved in the reactions leading to the formation of propene.

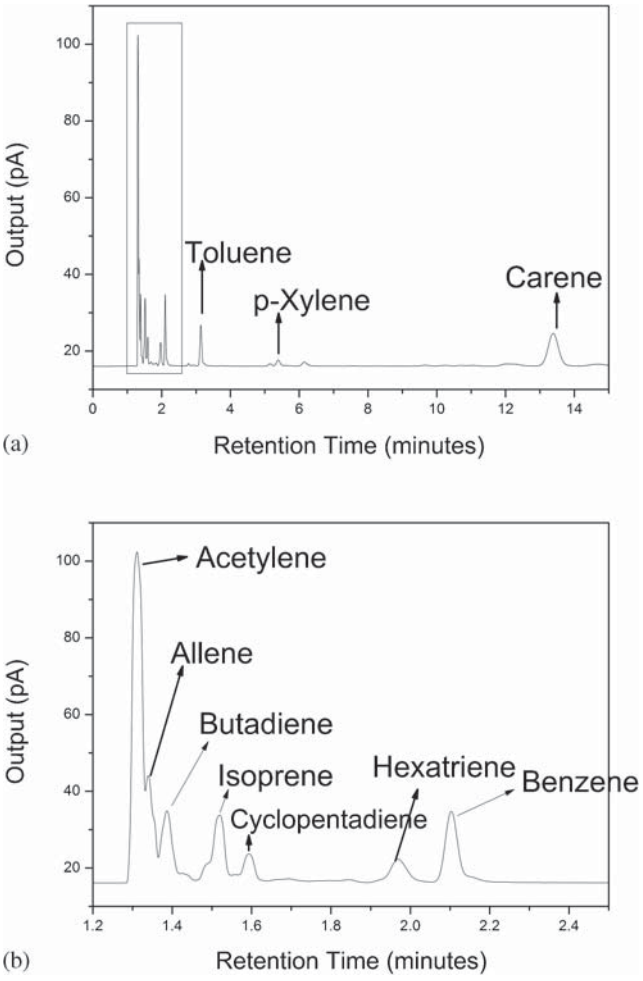

Figure 2. (a) Post shock chromatogram of 3-carene obtained in GC-FID. $T_5 = 1185$ K ; (b) The same chromatogram with time ranging from 1.2 to 2.5 min.

The peaks in the GC were identified and calibrated using standard sample except for three molecules, allene, cyclopentadiene and hexatriene. Standard samples for these could not be procured. Allene sensitivity was approximated to that of propyne. The presence of cyclopentadiene was also confirmed by the thermal decomposition studies of JP-10. It is well known that the pyrolysis of JP-10 will result in the formation of cyclopentadiene. The retention time of the peak corresponding to m/z=66 obtained in the thermal decomposition studies of 3-carene is the same as that of the

peak corresponding to m/z=66 obtained in the thermal decomposition of JP-10. To obtain the sensitivity of FID to hexatriene, we studied the relation between FID sensitivity and the number of C-H bonds present in C_6 molecules. A plot showing the variation of sensitivity with number of C-H present in the C_6 molecules is given in figure S1 in SI. Similar analysis was also carried out for cyclopentadiene. Its sensitivity was approximated to that of cyclopentene and appropriate reduction in sensitivity was done to account for the absence of two C-H bonds.

The initial concentration of 3-carene (pre-shock) was determined using GC. Since the post shock mixture will be diluted by helium (driver gas), one needs to find the amount of initial reaction concentration to which it is diluted. We have previously used the sum of all products and the final reactant concentration to estimate initial reaction concentration.[25] We have found this to be more accurate than the concentration measured initially. However, it is important to ensure that the all reactant and products have been recovered. Hence, the experimental conditions were chosen to avoid soot formation and condensation of reactants in the wall. Equation 2 has been used to obtain the initial concentration of the reactant as the uniformity and the extent of initial reactant concentration dilution were not known accurately. This was considered with an assumption that the entire carbon was recovered in the gaseous phase. The assumption can be justified on the backdrop of absence of soot formation even after all the experiments. The assumption can also be justified using the results from previous works where it has been found that below 1300 K, nearly 100% of carbon will recovered in gas phase.[30–32]

$$\begin{aligned}[\text{carene}]_0 = {} & (10 \times [\text{carene}]_t + 2 \times [\text{acetylene}]_t \\ & +3 \times [\text{allene}]_t + 4 \times [\text{butadiene}]_t \\ & +5 \times [\text{isoprene}]_t + 5 \times [\text{cyclopentadiene}]_t \\ & +6 \times [\text{hexatiene}]_t + 6 \times [\text{benzene}]_t \\ & +7 \times [\text{toluene}]_t \\ & +8 \times [\text{p}-\text{xylene}]_t)/10 \end{aligned} \quad (2)$$

Here, $[\text{carene}]_0$ is the initial concentration of 3-carene and $[\text{x}]_t$ is the concentration of the respective molecules after the reaction for a time t given in table 1.

The overall rate constant was calculated using Eq. 3. Arrhenius plot for overall decomposition of 3-carene is shown in figure 3.

$$k = -\frac{1}{t} \ln \frac{[carene]_t}{[carene]_0} \quad (3)$$

The rate constant expression shown in Eq. 4 was obtained by linear fitting the data in figure 3.

$$k/s^{-1} = 10^{(9.95 \pm 0.54)} e^{\frac{\left(-40.88 \pm 2.71/kcal.mol^{-1}\right)}{RT}} \quad (4)$$

The product concentrations indicate that the acetylene constitutes a major product in the dissociation of

Table 1. Summary of experimental conditions and normalized mole fraction of products obtained in pyrolysis experiments of 3-carene. T_1: Room temperature.

Exp. No.	Dwell Time ms	Temperature K	Pressure bar	C_2H_2	C_3H_4	C_4H_6	C_5H_8	C_6H_6	C_7H_8	C_8H_{10}	C_6H_8	C_5H_6	3-Carene
1	1.76	1151	12.15	0.238	0.067	0.063	0.058	0.027	0.036	0.017	0.032	0.011	0.799
2	1.65	974	8.71	0.003	0.001	0.001	0.002	0	0.001	0	0.001	0.008	0.992
3	1.66	1038	9.17	0.01	0.005	0.004	0.01	0.001	0.003	0.001	0.003	0	0.985
4	1.53	1163	11.02	0.2	0.071	0.062	0.071	0.017	0.029	0.016	0.035	0.008	0.81
5	1.72	1057	9.5	0.019	0.008	0.006	0.015	0.001	0.005	0.003	0.006	0.002	0.973
6	1.5	1220	13.48	0.866	0.209	0.189	0.1	0.088	0.082	0.032	0.054	0.037	0.451
7	1.65	1172	14.66	0.4	0.128	0.103	0.106	0.033	0.056	0.026	0.056	0.036	0.656
8	1.57	1172	15.26	0.373	0.111	0.095	0.101	0.029	0.053	0.027	0.06	0.037	0.673
9	1.48	1198	11.67	0.455	0.132	0.108	0.081	0.052	0.064	0.025	0.041	0.022	0.655
10	1.64	1066	9.87	0.034	0.015	0.013	0.025	0.002	0.009	0.004	0.012	0.003	0.951
11	1.61	1136	10.35	0.19	0.071	0.059	0.082	0.013	0.036	0.018	0.045	0.02	0.791
12	1.55	1101	11.27	0.094	0.035	0.031	0.033	0.041	0.019	0.009	0.023	0.004	0.881
13	1.49	1163	12.83	0.396	0.087	0.079	0.066	0.04	0.038	0.017	0.04	0.025	0.73
14	1.4	1027	11.03	0.015	0.005	0.006	0.013	0.004	0.005	0.001	0.006	0	0.976
15	1.4	1009	11.1	0.01	0.003	0.004	0.008	0.004	0.003	0.001	0.004	0	0.984
16	1.39	1066	11.17	0.045	0.018	0.019	0.035	0.005	0.008	0.005	0.019	0	0.937
17	1.35	926	8.69	0.003	0.001	0.001	0.001	0.002	0.002	0	0.003	0	0.994
18	1.57	1150	13.35	0.347	0.099	0.131	0.095	0.032	0.041	0.021	0.054	0.025	0.692

Here, C_2H_2: Acetylene, C_3H_4: Allene, C_4H_6: Butadiene, C_5H_8: Isoprene, C_5H_6: Cyclopentadiene, C_6H_6: Benzene, C_7H_8: Toluene, C_8H_{10} = p-Xylene, C_6H_8: Hexatriene.

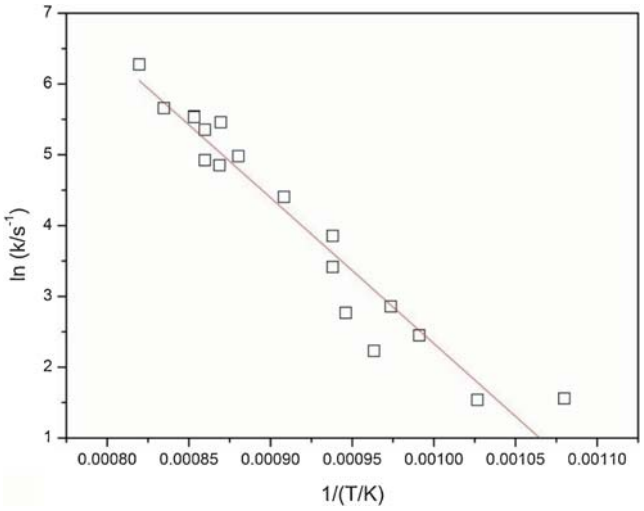

Figure 3. Arrhenius plot for overall decomposition of 3-carene.

3-carene. Allene, butadiene and isoprene were the next major products and these are equally important. Among the minor products, [Toluene] > [Benzene] > [Hexatriene] > [p-Xylene]. The conditions at which experiments were carried out and the normalized product mole fractions have been given in table 1. The available literature[13] on 3-carene thermal decomposition for temperature ranging from 723 to 948 K indicated the formation of aromatic compounds as major products. 3-carene started to crack at 723 K and at 753 K, one third 3-carene got converted into products. At 833 K, the entire 3-carene concentration was converted into products. In the above said range (753 to 833 K), toluene, xylene, and cymene were the major constituents of the observed products followed by methylstyrene, styrene, benzene and dehydrocymene. Isoprene and propene were minor products. In the present work, we observed around 40% of acetylene. Allene, butadiene and isoprene together were found to constitute 30% of the product concentration. Hexatriene, toluene, xylene and benzene account for the rest.

Pyrolysis studies of isoprene which was carried out for temperature ranging from 673 to 1273 K resulted in the formation of 49 aromatic products with several PAHs.[20] Pyrolysis of isoprene at 973 K resulted in the formation of benzene, toluene and xylene as major products and accounted for 52% of the observed products.[21] Flash pyrolysis of isoprene resulted in the formation of linear molecules and benzene was observed after 1250 K.[22] On careful observation, a similar behaviour can also be observed in the pyrolysis of 3-carene. The observed aromatic molecules at lower temperatures (and longer time) and linear molecules at higher temperatures (for test time comparable to that of flash pyrolysis) suggests a similar behavior by 3-carene as that of isoprene. The aromatic products observed in isoprene thermal decomposition were also observed in our experiments. The molecular formula for 3-carene, $C_{10}H_{16}$ happens to be twice that of isoprene, C_5H_8. However, structurally they are very different and 3-carene is not formed by combining two isoprene units. However, isoprene is one of the products from its decomposition process. Hence, we explored the possibility of isoprene being the primary product and formation of other products through isoprene decomposition. The differences in molecular structure clearly suggests that direct formation of isoprene from 3-carene is not possible. Moreover, the observed product profiles also indicate that this pathway is not likely. For example, the minimum energy pathway leading to the formation of acetylene from isoprene involves its decomposition to propene and vinylidine, which has a barrier of 92.3 kcal mol^{-1} and will not yield the observed acetylene concentration. However, in the present work we have found that at lower temperatures (<1050 K) the concentrations of isoprene and acetylene are almost equal and with increase in temperature, the concentration of acetylene was found to increase more rapidly compared to that of isoprene. Cyclopentadiene, which was recently proposed as one of the precursor for PAH[33] was observed to form after 1150 K.

All the observed products distribution indicates that the primary product should be a linear molecule and not cyclic. Cocker *et al.*[13] in particular discussed the resistance of cyclopropane ring present in 3-carene to decompose in vapor phase. This has a minimum BDE compared to rest of the bonds in 3-carene. The path leading to the formation of observed products will be explained in theoretical and mechanism sections.

3.2 *Theoretical Observations*

Ab-initio theoretical calculations were carried out to find the minimum energy pathway that could lead to the formation of experimentally observed products. Transition states (TS) were optimized to find the energy barrier involved in the reactions. The theoretical rate constants were calculated using Eq. 5.

$$k = l\frac{k_B T}{h} \times \frac{Q^{\neq}}{Q_R} \times e^{-\frac{E_a}{RT}} \tag{5}$$

Here, Q_R and $Q^{\#}$ correspond to partition functions for reactant and activated complex, respectively. T is temperature, E_a is activation energy, K_B is Boltzmann constant, l is reaction degeneracy factor.

Partition functions were calculated using the vibrational frequencies and rotational constants obtained at

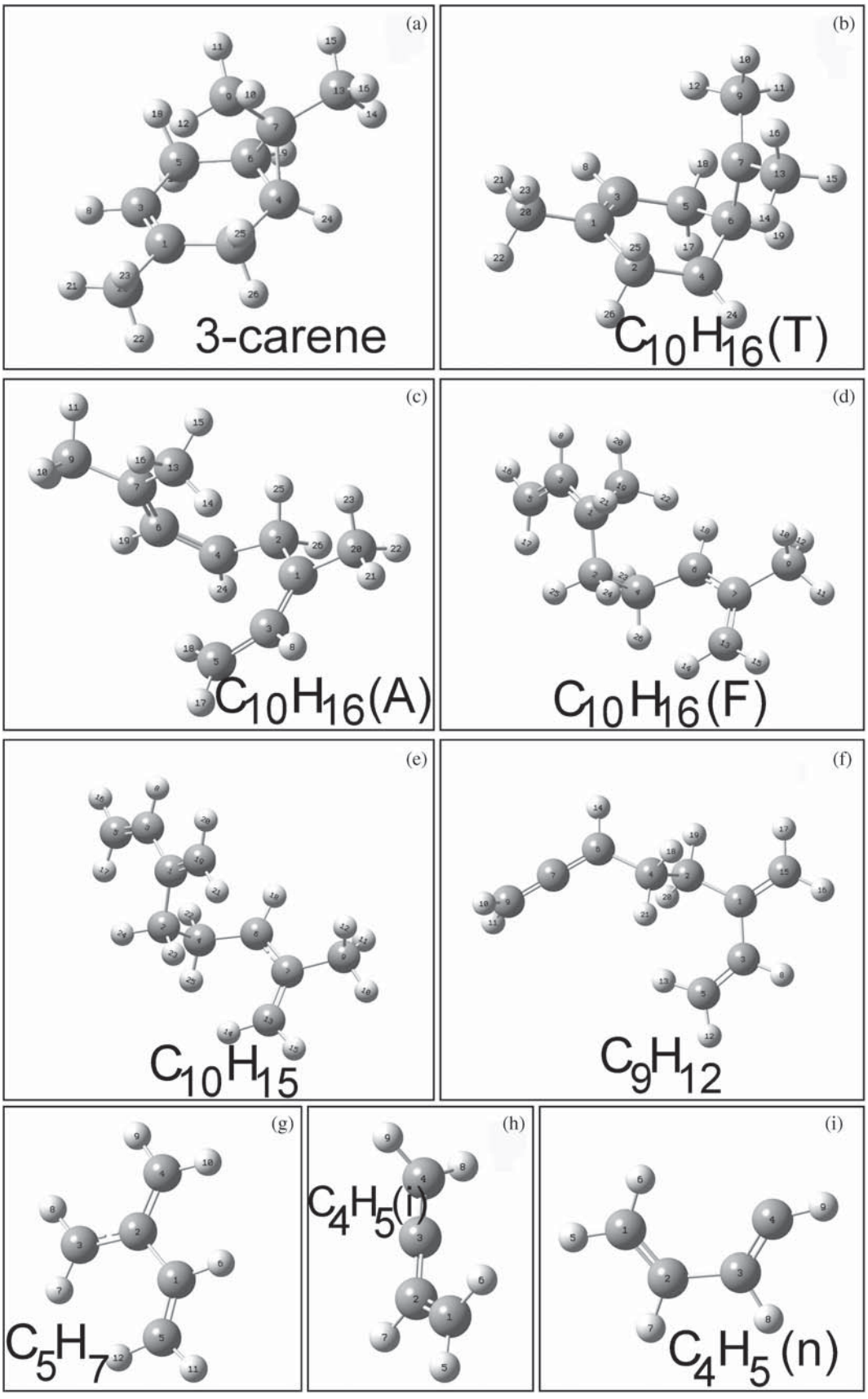

Figure 4. Molecular structure of 3-carene and intermediates formed in the thermal decomposition of 3-carene optimized at G3 level of theory. Here, (a) and (f) are in singlet state, (b), (c) and (d) are in triplet state and, (e), (g), (h) and (i) are in doublet state.

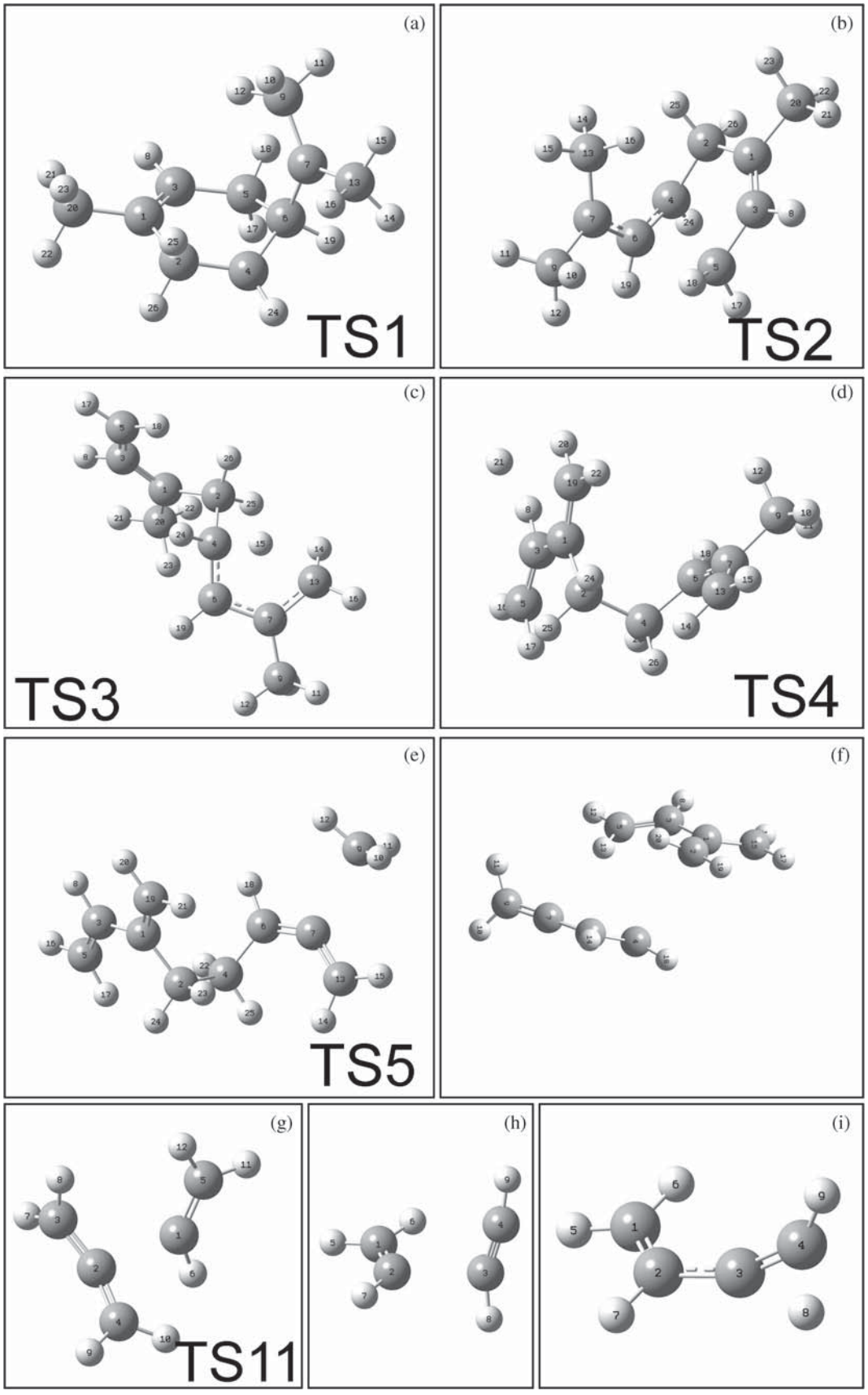

Figure 5. Transition state structures for intermediate reaction steps originating from 3-carene optimized at G3 level of theory (except for TS1, optimized at B3LYP/6-311+G(d,p) level of theory.

B3LYP/6-311+G(d,p) level of theory. The obtained rate parameters are summarized in table S3.

The following section describes the decomposition pathways of 3-carene. The pathways involving radicals formed from the H-dissociation and H-abstraction from 3-carene will also be discussed.

3.2.1 *3-Carene Decomposition Pathways:* The formation of linear molecules even at low temperatures indicates that 3-carene ring structure should form a linear molecule/intermediate in the initial stages of its dissociation process. Theoretical calculations also support the above statement. The theoretically optimized molecular/intermediate structures which will be described in this section are shown in figure 4. The transition state structures which were optimized to find the minimum energy path for the reactions are shown in figure 5.

3.2.1a *3-carene ring opening and rearrangement:* Except for the first step, all TS (transition state) energies were calculated at G3 and B3LYP/6-311+G(d,p) level of theories. The first step, formation of di-radical, structure of which has been shown in figure 4(b), $C_{10}H_{16}$(T), was analyzed using only B3LYP/6-311+G(d,p) level of theory. Attempts to optimize transition state structure at MP2/6-31G* level of theory were not successful. The energy barrier for the above reaction was found to be 51.0 kcal mol^{-1}. The potential energy scans for all C-C and C=C bonds are shown in figure S2, given in the Supplementary Information. It was clear that the dissociation barriers for C-C and C=C bonds are >80 kcal mol^{-1}. The BDE (Bond dissociation Energy) for C7-C13 bond is 83 kcal mol^{-1}. The C-H BDEs and, the barriers involved in H abstraction from 3-carene by an H atom have been shown in figure 6. Hence the structure shown in figure 4(b) has been considered as the first intermediate from thermal decomposition of 3-carene.

The C5-C6 bond (in $C_{10}H_{16}$(T)) shown in figure 4(b) has a BDE of 14.8 (23.3) kcal mol^{-1} at B3LYP/6-311+G(d,p) (G3) level of theory. The ring opening process will lead to the formation of a linear intermediate, $C_{10}H_{16}$(A), the structure shown in figure 4(c). The H migration to form structure shown in figure S3, given in the Supplementary Information is not considered as it has a higher barrier. At B3LYP/6-311+G(d,p) level of theory the difference between ring opening and H migration is 18.4 kcal mol^{-1}. Also, the rate constants for ring opening process at 1000 K, 3.7 × 10^{9} s^{-1}, can be compared with 2.8 × 10^{5} s^{-1}, for the H migration process. The potential energy scans along C-C stretching in the intermediate structure given in figure 4(b) showed that the considered reaction path has the least energy barrier compared to the rest of the C-C bonds. The C=C BDE is assumed to be >C-C BDE. Hence, the formation of the linear intermediate shown in figure 4(c) from the structure shown in figure 4(b) was found to have a lower BDE and can explain the formation of observed products. The potential energy scans along C-C stretching for the structure shown in figure 4(b) has been given in figures S4 and S5 in the Supplementary Information.

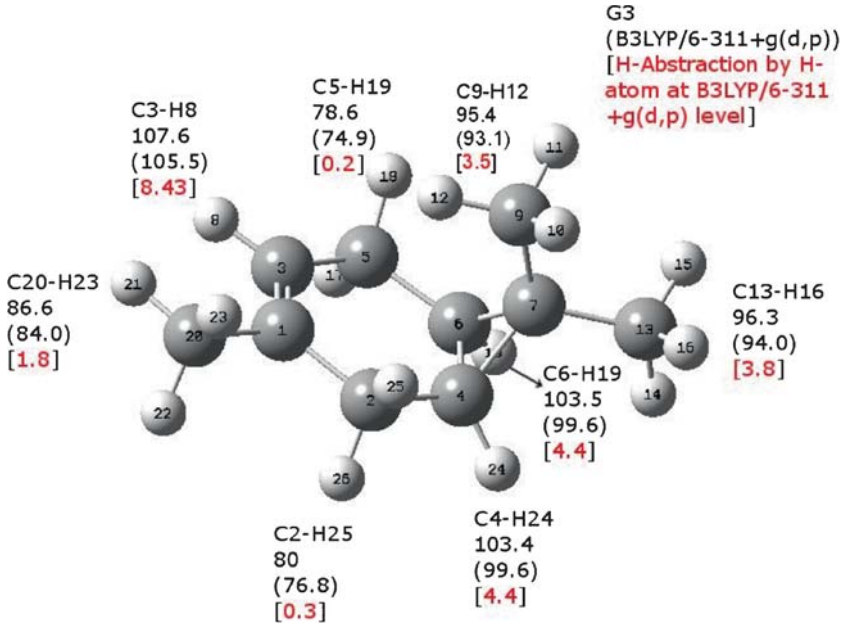

Figure 6. C-H BDEs at G3 and B3LYP/6-311+G(d,p) level of theories and barriers involved in H abstraction in 3-carene by an H atom.

The hydrogen H14 in the structure, $C_{10}H_{16}$(A), shown in figure 4(c) migrates from C13 carbon to C4 carbon forming a structure, $C_{10}H_{16}$(F), looking like dimer of isoprene shown in figure 4(d). The activation energy for the above mentioned reaction is 32.9 (36.7) kcal mol^{-1} at B3LYP/6-311+G(d,p) (G3) level of theory. The C-C and C-H BDEs for the structure shown in figure 4(c) are given in table S3. The rate constant for C20-H23 bond dissociation reaction was found (at 1000 K) to be an order lower than that of H migration reaction. Similar differences were also found for C13-H15 and C9-H12 dissociation reactions. Even though the C2-H26 BDE is very close to that of H migration reaction, the subsequent reaction from the radical formed by C2-H26 bond dissociation will lead to a C_{10} molecule, which is not observed in the present experiment and hence not considered in the kinetic mechanism presented in the paper.

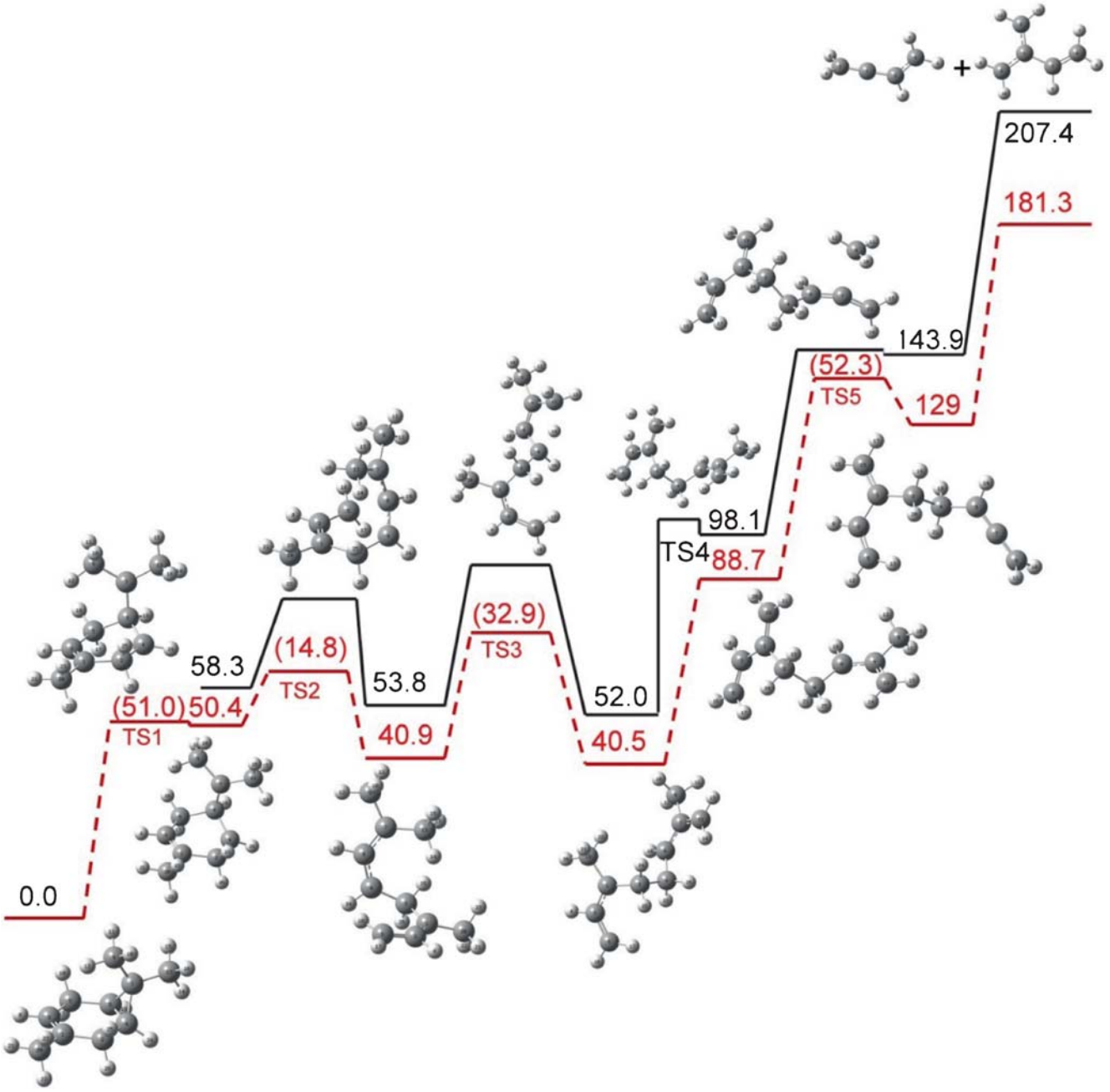

Figure 7. Schematic diagram depicting energies of molecules, intermediates and transition states involved in 3-carene decomposition. Solid lines (Black): G3 level of theory, Dotted lines (Red): B3LYP/6-311+G(d,p) level of theory. The values given in the parenthesis correspond to transition state energy of the corresponding reaction.

3.2.1b *Formation of lower hydrocarbons:* The dissociation of hydrogen from C19 carbon in structure shown in figure 4(d) results in the formation of $C_{10}H_{15}$, structure of which has been shown in figure 4(e). The barrier for the above reaction at B3LYP/6-311+G(d,p) (G3) level of theory is 48.2(50.2) kcal mol^{-1}. The C-C BDEs for the structure shown in figure 4(d) has been summarized in table S4. The reactions involving radicals formed from H dissociation from C2 and C4 [$C_{10}H_{15}$(FH1) in figure 8] carbon atoms will be discussed later in this paper. Formation of isoprene from the structure shown in figure 4(d) preceded by CH_3 elimination (C7-C9 bond dissociation) is not considered in the mechanism as the detailed analysis showed

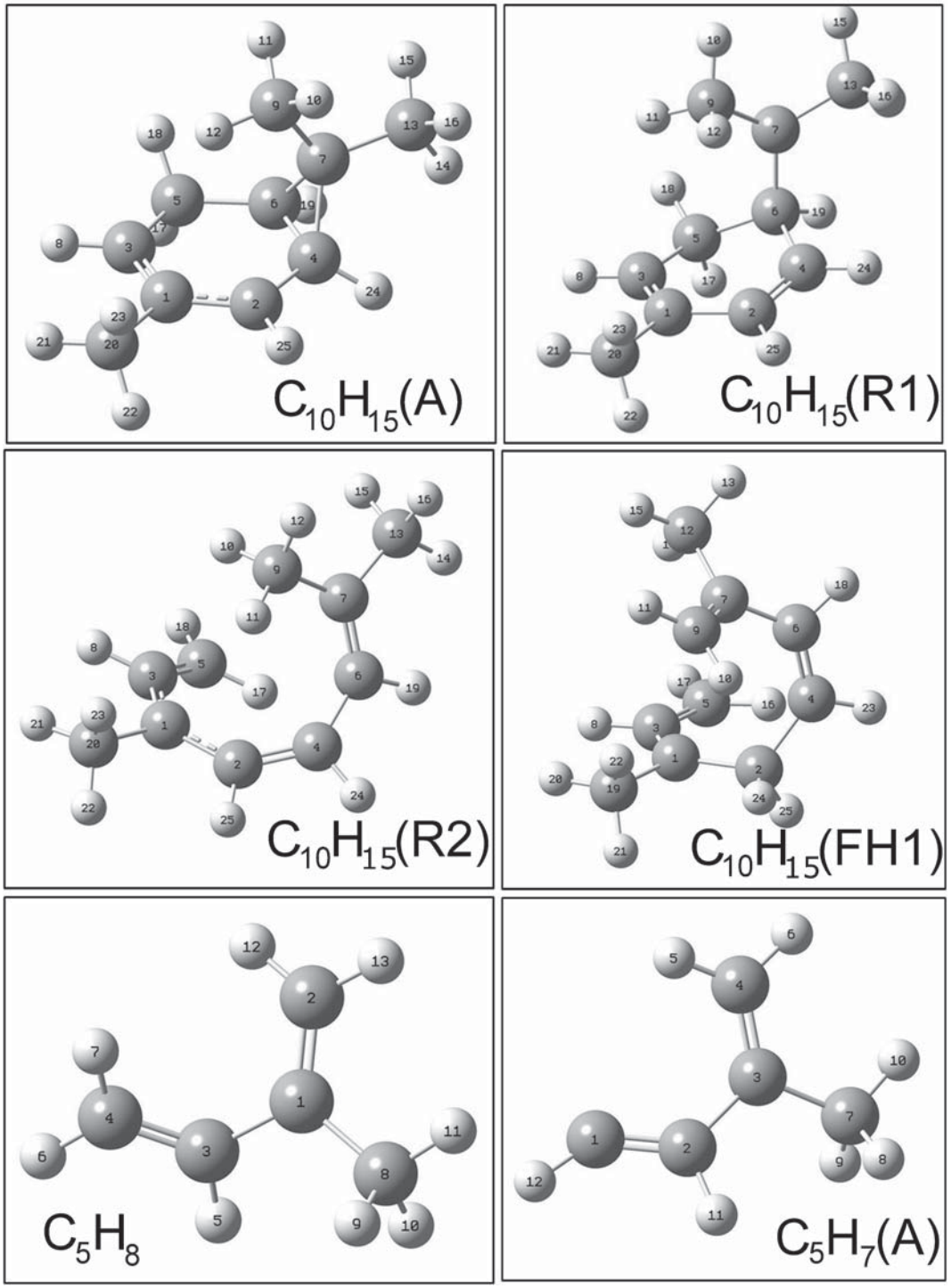

Figure 8. Molecular structure of 3-carene radical ($C_{10}H_{15}$ (A)) and intermediates formed in the decomposition of 3-carene-H radical ($C_{10}H_{15}$ (A)) optimized at G3 level of theory.

that the barrier involved in the dissociation of C7-C9 is ∼60 kcal mol^{-1} at B3LYP/6-311+G(d,p) level of theory. The potential energy scan along the above said C-C stretching is shown in figure S7 in the Supplementary Information.

The doublet $C_{10}H_{15}$, structure of which is shown in figure 4(e) then looses CH_3 group to form C_9H_{12} (figure 4(f)). The BDE of C7-C9 decomposition at B3LYP/6-311+G(d,p) (G3) level of theory is 52.3(59.7) kcal mol^{-1}. The BDE of C4-C6 bond at B3LYP/6-311+G(d,p) (G3) level of theory is 59.4 (64.5) kcal mol^{-1}. However the scan along C4-C6 bond showed that barrier involved in the C4-C6 dissociation at B3LYP/6-311+G(d,p) level of theory is greater than

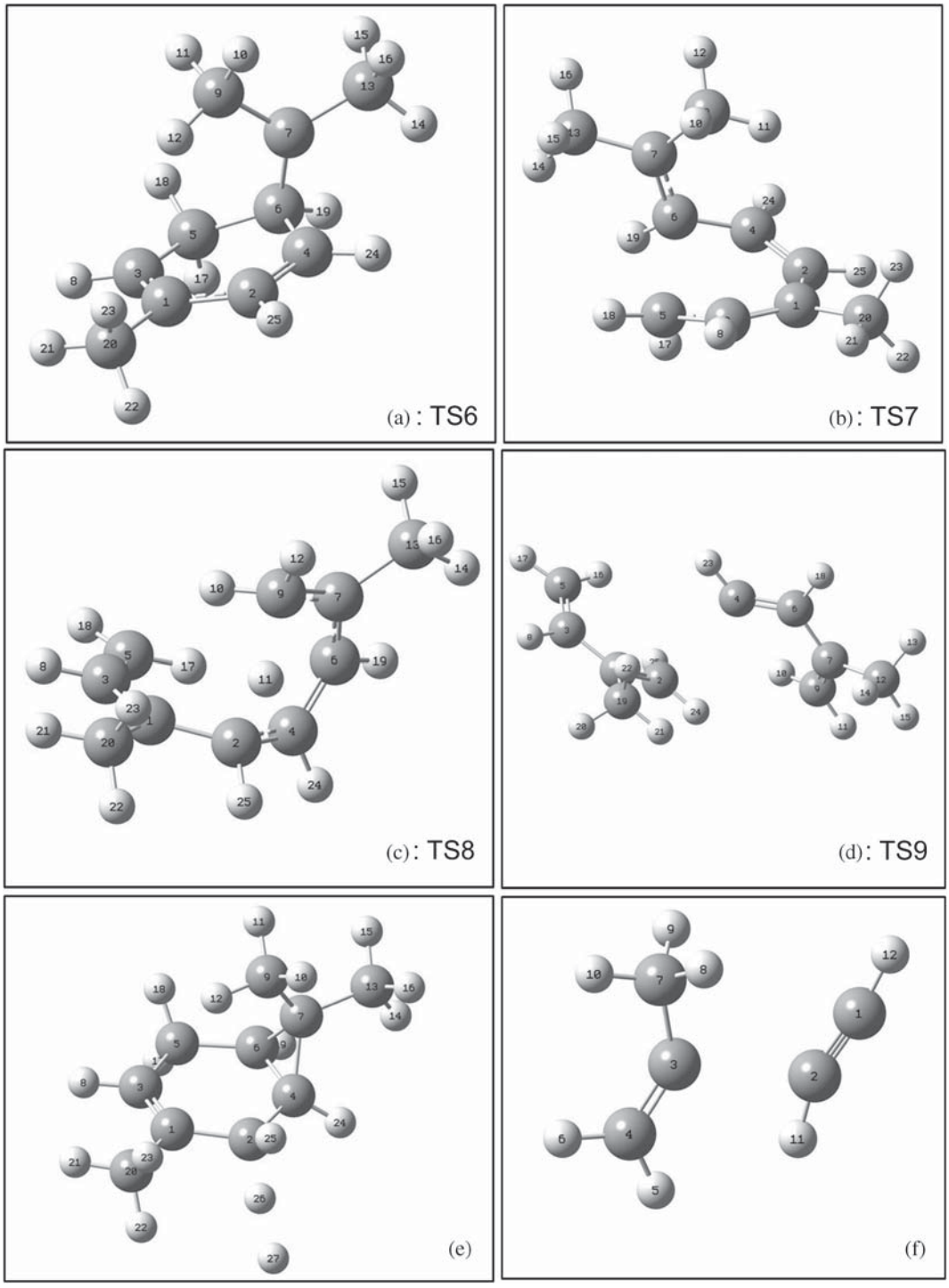

Figure 9. Transition state structures for intermediate reaction steps originating from 3-carene radical ($C_{10}H_{15}$ (A)) optimized at G3 level of theory.

85 kcal mol^{-1}. The BDE of C2-C4 bond (at B3LYP/6-311+G(d,p) (G3) level of theory) in the structure shown in figure 4(f) is 52.3(63.5) kcal mol^{-1}. This bond dissociation will lead to the formation of isoprene radical (figure 4(g)) and butadiene radical (figure 4(h)). The BDE of C4-C6 bond (at B3LYP/6-311+G(d,p) level of theory), the dissociation of which results in the formation of allene radical is 69.9 kcal mol^{-1} and hence not considered in the mechanism presented in this paper. The schematic diagram showing the relative energies of the transition state, intermediates and products are given in figure 7. The transition state energies given in the figure are calculated at B3LYP/6-311+G(d,p) level of theory. The transition state energies for same reactions/steps are given in table S5.

3.2.2 *$C_{10}H_{15}$ Decomposition Pathway:* The structures of the radicals formed after H dissociation and H abstraction from 3-carene and, transition state structures for H abstraction have been given in figures S8 and S9. It has been found that the pathways leading from carene-H(A)($C_{10}H_{15}$(A)), formed from H removal at C2 site, and carene-H(B)($C_{10}H_{15}$(B)), formed from H removal at C5 site, play important roles in the dissociation of 3-carene. The pathways leading from other radicals formed by H dissociation/abstraction at other carbon site can be neglected as the barriers involved in the H dissociation/abstraction and subsequent dissociation leading to the products were found to be higher when compared to $C_{10}H_{15}$ (A) and $C_{10}H_{15}$(B) dissociation pathways.

In this paper the reaction pathway originating from radicals formed by C2-H26 dissociation/ H26-H abstraction will be described. The intermediate structures involved in the decomposition pathways of $C_{10}H_{15}$(A) are shown in figure 8. The transition states involved in the decomposition pathways of $C_{10}H_{15}$(A) are shown in figure 9.

The dissociation pathways of $C_{10}H_{15}$(A), shown in figure 8(a), are similar to that of 3-carene. As in 3-carene, the first step was found to be C_3 ring opening process and will lead to the formation of $C_{10}H_{15}$(R1), shown in figure 8(b). The energy barrier involved in the reaction at B3LYP/6-311+G (d,p) (G3) level of theory is 10.2 (15.9) kcal mol^{-1} and the transition state structure for the reaction is shown in figure 9(a). The dissociation of C5-C6 bond in $C_{10}H_{15}$ (R1) leading to the formation of $C_{10}H_{15}$ (R2) has a barrier of 18.7 (27.0) kcal mol^{-1} at B3LYP/6-311+G(d,p) (G3) level of

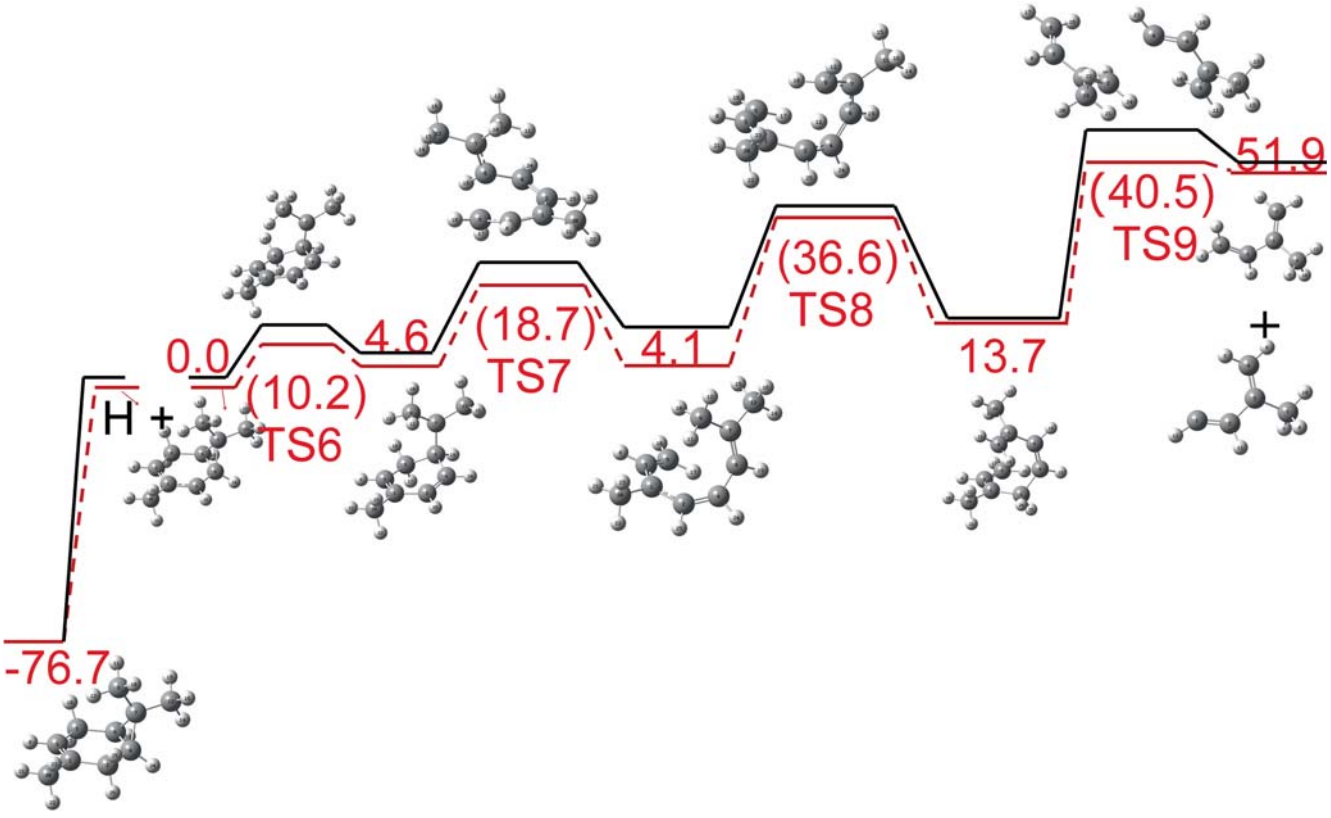

Figure 10. Schematic diagram depicting energies of molecules, intermediates and transition states involved in 3-carene radical ($C_{10}H_{15}$ (A)) decomposition. Solid lines (Black): G3 level of theory, Dotted lines (Red): B3LYP/6-311+G (d,p) level of theory. The values given in the parenthesis correspond to transition state energy of corresponding reaction.

theory and the transition state structure is shown in figure 9(b). The above step is similar to ring opening process leading to $C_{10}H_{16}$ (A) from $C_{10}H_{16}$(T).

The third step as for 3-carene is H-migration. The hydrogen migration from C9 to C2 carbon atom leading to $C_{10}H_{15}$ (FH1), shown in figure 8, has a barrier of 36.6 (36.5) kcal mol^{-1} at B3LYP/6-311+G(d,p)(G3) level of theory. The transition state structure for the above reaction is shown in figure 9(c). Unlike 3-carene, the next step in the dissociation was found to be C2-C4 bond dissociation resulting in the formation of isoprene, C_5H_8, and C_5H_7 (A) radical. The transition state structure for the above reaction is shown in figure 9(d). The reaction step has a barrier of 40.5 (57.2) kcal mol^{-1} at B3LYP/6-311+G(d,p) (G3) level of theory. The C3-C2 bond dissociation in C_5H_7 (A) leading to acetylene and C_3H_5 has a BDE of 35.9 (40.9) kcal mol^{-1} at B3LYP/6-311+G(d,p)(G3) level of theory. The transition state structure for the above reaction is given in figure 9(f). The transition state structure for H26 abstraction by H atom is shown in figure 9(e). The schematics showing the relative energies of transition states and intermediates with respect to $C_{10}H_{15}$ (A) is shown in figure 10. The reaction pathway originating from $C_{10}H_{15}$ (B) was found to be similar to that of $C_{10}H_{15}$ (A) and hence not described in detail. However schematics showing the relative energies of intermediates, transition states and products calculated at B3LYP/6-311+G (d,p) level of theory is given in figure S11 in the Supplementary Information.

Even though the BDE of rest of C-H bonds in 3-carene is higher than those of above discussed C-H bonds, for the sake of completion, results of the calculations which were carried out to understand the decomposition pathways of rest of the radicals formed by H dissociation/abstraction at other carbon sites will be briefly described below. The potential energy scans of the bonds which will be discussed below are given in the Supplementary Information (figures S13-S15).

The final products from the dissociation of radicals formed by the H dissociation/abstraction of hydrogen at C9 ($C_{10}H_{15}$(C)) and C13 ($C_{10}H_{15}$ (D)) sites in 3-carene are same as those of $C_{10}H_{15}$ (A) and $C_{10}H_{15}$ (B). The first and second step like 3-carene are C_3 ring opening and C5-C6 bond dissociation (to form a linear structure from ring structure), respectively. However in the case of $C_{10}H_{15}$(C) and $C_{10}H_{15}$ (D) the H migration reaction is not required to form the final products. The barrier involved in the second ring opening process leading to a linear intermediate from ring structure was higher than those of $C_{10}H_{15}$ (A) and $C_{10}H_{15}$(B) second ring opening process. Dissociation of C2-C4 bond in the resulting structure will lead to the formation of isoprene, C_5H_8, and C_5H_7 (A) radical.

The radical formed by H dissociation/abstraction from C20 site ($C_{10}H_{15}$ (E)) in 3-carene, which has a BDE closer to C-H BDE to form $C_{10}H_{15}$ (A) and $C_{10}H_{15}$(B) from 3-carene, has a different dissociation pathway than those explained above. In this case the first step of dissociation process is breaking of C1-C2 bond. A series of dissociation reactions result in the formation of C_3H_3 and C_7 molecules. The energy barriers involved in the dissociation process of $C_{10}H_{15}$ (E) is considerably higher than those of $C_{10}H_{15}$ (A) and

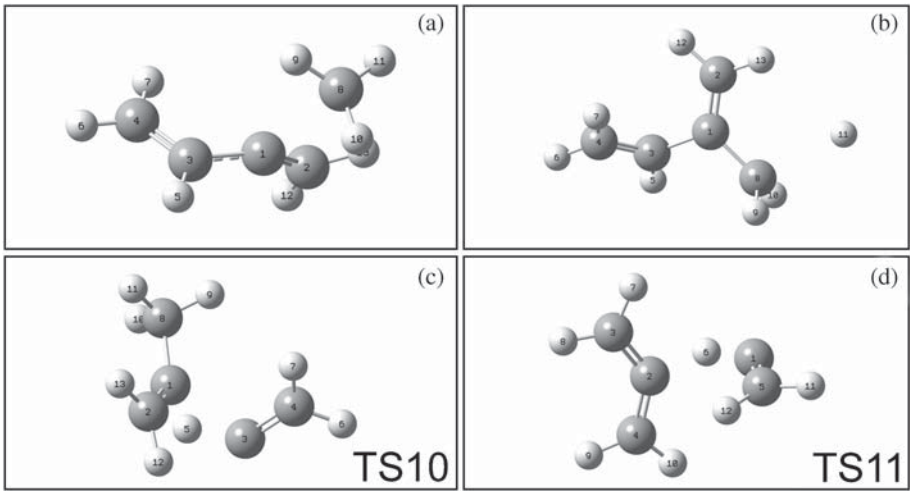

Figure 11. Transition state geometries for (a) CH_3 decomposition from isoprene; (b) Hydrogen dissociation from isoprene to form isoprene radical; (c) Propene molecular elimination from isoprene; and (d) C_3H_5 + vinyldiene elimination from isoprene radical optimized at G3 level of theory.

C10H15 (B). A detailed pathway for $C_{10}H_{15}$ (E) dissociation has been given in the Supplementary Information.

The H dissociation/abstraction from C4 ($C_{10}H_{15}$ (F)) and C6 ($C_{10}H_{15}$ (G)) sites in 3-carene followed by breaking of C6-C7 and C4-C7 bonds, respectively, was also analyzed in our study. The C6-C7 and C4-C7 dissociation reactions are exothermic ($\sim$ 30 kcal mol^{-1}). However, the above explained exothermic reaction will lead to a structure with a higher C-C and C-H BDEs. The C1-C2 (C3-C5) bond dissociation in $C_{10}H_{15}$ (F) ($C_{10}H_{15}$ (G)), even though an endothermic reaction, can result in the formation propyne and C_5 intermediate with a lower energy bottle neck. The potential energy scans leading to propyne from C_8 intermediate has been given in figure S15 in the Supplementary Information.

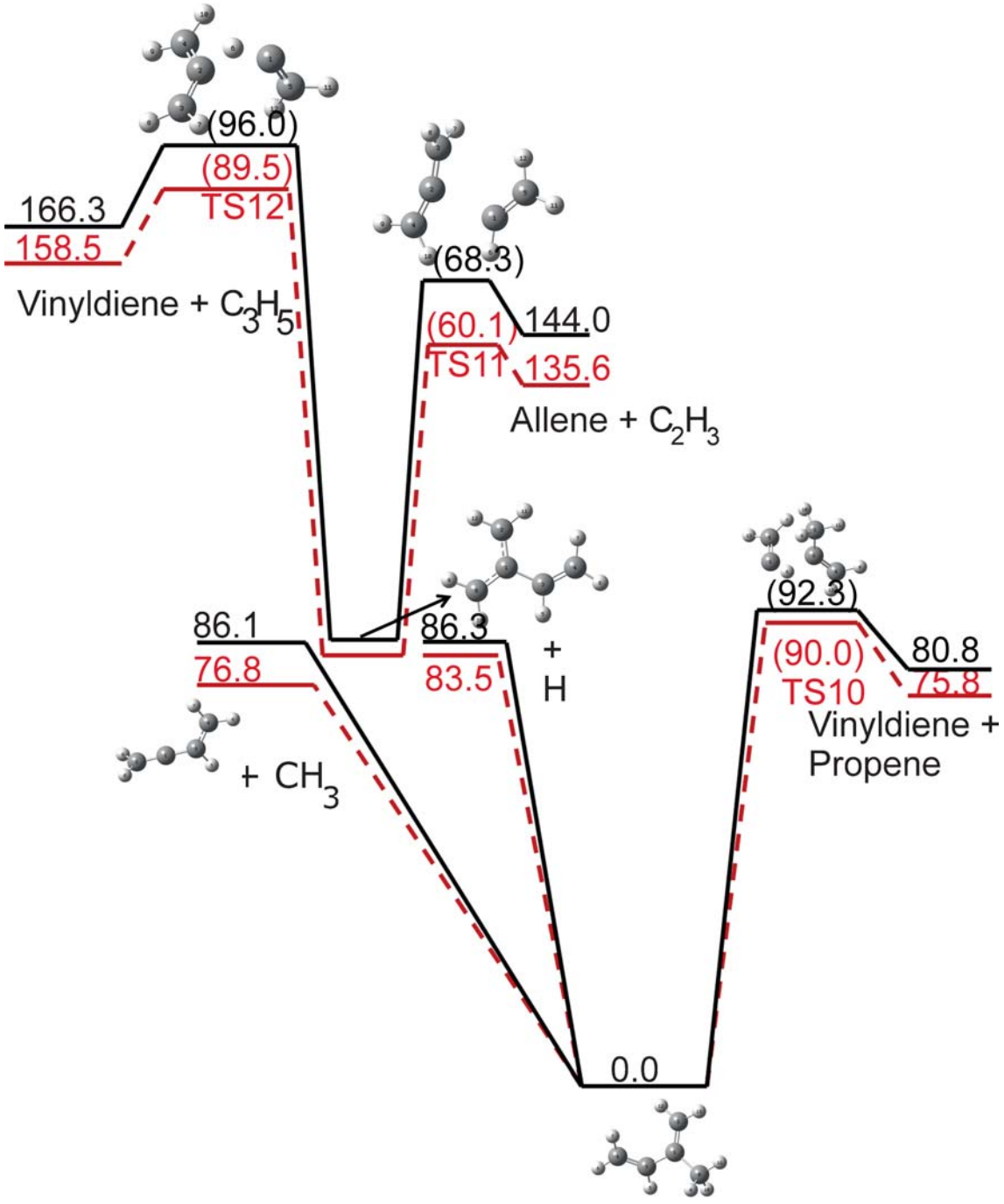

Figure 12. Schematic diagram depicting energies of molecules, intermediates and transition states involved in isoprene decomposition. Solid lines (Black): G3 level of theory, Dotted lines (Red): B3LYP/6-311+G(d,p) level of theory.

3.2.3 *Isoprene Decomposition Pathway:* Formation of isoprene radical from 3-carene and, isoprene from $C_{10}H_{15}$ (A) and $C_{10}H_{15}$ (B), respectively, necessitated the decomposition study of isoprene molecule. Transition states for two molecular elimination pathways, one each for isoprene and isoprene radical, have been found. The reaction which leads to the formation of propene and vinylidine from isoprene has an energy barrier of 90.0 (92.3) kcal mol^{-1} at B3LYP/6-311+G (d,p) (G3) level of theory. The transition state structure for the above reaction is shown in figure 11(c). The reaction leading to the formation of CH_2CHCH_2 and vinylidene from isoprene radical has a barrier of 89.5 (96.0) kcal mol^{-1} at B3LYP/6-311+G (d,p) (G3) level of theory. The transition state structure for the above mentioned step is shown in figure 11(d). The C2-C1 bond dissociation in isoprene radical was found to result in the formation of allene and vinyl radical. The above reaction has a barrier of 60.1 (68.3) kcal mol^{-1} at B3LYP/6-311+G (d,p) (G3) level of theory. This reaction was found to explain the formation of the observed C_3 molecule concentration. Since the reactant for the

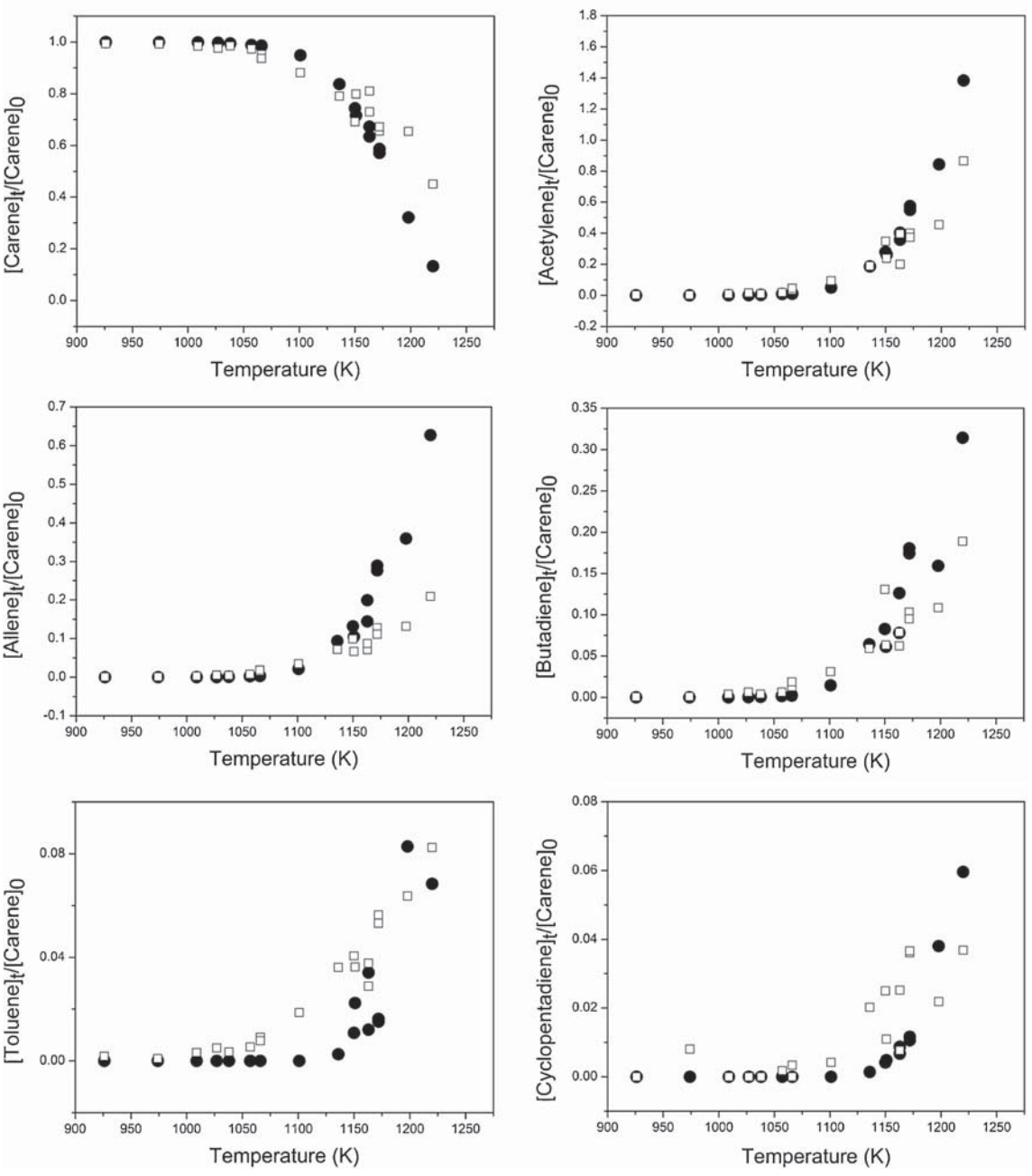

Figure 13. Normalized concentration profiles of selected molecules with temperature. squares: Experimental values. circles: Values obtained from the mechanism.

above step is formed in the decomposition of 3-carene, transition state structure for the above reaction is also given in the figure 5(g). A schematic diagram showing relative energies of reactant, intermediates and transition states with respect to isoprene energy has been given in figure 12.

3.3 *Kinetic Mechanism*

With the help of results described in experimental and theoretical sections, the mechanism for the 3-carene thermal decomposition given in table S2, with 44 reactions involving 37 species, has been derived to fit the product concentrations observed in the present experimental work. Since a mechanism for pyrolysis of both 3-carene and isoprene does not exist in the literature, we have tried to use minimum number of reactions to explain the product profiles observed in the present experiments.

After simulating the mechanism, given in table S2, at reaction conditions given in table 1, it was again simulated at 300 K and 2 atm for 10 ms. This has been done to take into account of radical reactions which can continue until all are consumed. The rate parameters used in the mechanism are obtained from TST calculations and refined to fit the observed concentrations. For simple molecular systems, such refinements in TST rate parameters may not be required. However in the present case, even with such a detailed analysis for the considered system we could not explain the observed product concentrations without such small variations in the calculated theoretical rate parameters. To compare the rate parameters calculated using TST at B3LYP/6-311+G(d,p) level of theory and the one used in the mechanism, the former is also given in table S3.

The rate constant for reaction R9 was obtained using the literature and the present work. Pre-exponential factor was obtained using the variational transition state theory and the activation energy was obtained using reported work.[34] The pre-exponential factor for R14 was increased from 6.16×10^{11} to 1.00×10^{12} cm^3 $mole^{-1}$ s^{-1}. The Arrhenius rate parameters, 9.77×10^{12} cm^3 $mole^{-1}$ s^{-1} and 0.1 kcal mol^{-1} given in the literature[35] for reaction R16 can be compared with present values of 6.0×10^{14} cm^3 $mole^{-1}$ s^{-1} and 0.1 kcal mol^{-1}. The n factor used the literature for R16 is -0.08 while in the present work we have used n factor of 0.7 for the same.

Pre-exponential factor for R25 was increased from 1.38×10^{13} to 6.0×10^{13} cm^3 $mole^{-1}$ s^{-1}. We are unable to explain xylene formation through transition state theory. Since isoprene decomposition also resulted in the formation of xylene, and, previous results of isoprene decomposition showed the formation of allene, we are proposing the following reaction to explain the formation of xylene.

$$[R26]\ C_5H_7 + C_3H_4 = C_8H_{10} + H$$

Reactions R17 and R18 were included to check whether xylene could be a secondary product formed by reaction of toluene and CH_3 radical. For Reaction R17, a range of rate constants in the literature were also considered. The rate constant for the reaction was varied in the available data range to find out its effect on xylene formation. The recombination rate constant for R19 was approximated to the following reaction.

$$[R25]\ C_6H_5 + CH_3 = C_6H_5CH_3$$

The obtained results suggested that the reactions R17 and R18 will not be able to explain xylene concentration obtained in the present experimental work. Thus, xylene could have formed through reaction R26. Rate constant for the above reaction was fitted to obtain the observed xylene concentration. One more possible pathway for xylene formation could be that of C_4H_5 dimerisation process, but, it is not considered in the present work. The comparison of concentrations obtained in experiments and simulation is given in figure 13 and the results are in reasonable agreement.

4. Conclusions

Thermal decomposition experiments of 3-carene have been carried out for temperatures ranging from 920 to 1220 K. Linear products were found to form in major concentrations. *Ab initio* calculations were carried out to help in deriving and understanding the pyrolysis mechanism of 3-carene. Opening of C_3 ring in 3-carene as well as in $C_{10}H_{15}$(A) and $C_{10}H_{15}$(B) was found to be the first step in their decomposition process. Theoretical calculations also showed that 3-carene decomposition will lead to the formation of linear products. Rate parameters obtained using transition state theory was refined and used in the kinetic mechanism presented in the paper. The mechanism fairly replicated the formation of observed product concentration. This is the first detailed experimental and theoretical work carried out on 3-carene decomposition process. We hope that this work will help in deriving the oxidation mechanism and, stimulate further experimental and theoretical studies on the pyrolysis of this important molecule.

Supplementary Information

Full citation for Ref 27., sensitivity of FID to the molecules, tables S1-S6, selected potential energy

scans, structures of diradical-2, 3-carene-H radicals and TS for H abstraction at different sites in 3-carene, Pathways for dissociation of 3-carene-H radicals, cartesian coordinates and normal mode frequencies of molecules, intermediates and transition states are given in Supplementary Information which is available at www.ias.ac.in/chemsci.

Acknowledgements

We acknowledge funding from the following organizations: IISc-ISRO Space Technology Cell, Defence Research Development Organization, Defence Research Development Laboratory and Aeronautics Research and Development Board.

References

1. Granata S, Faravelli T and Ranzi E 2003 *Combust. Flame* **132** 533
2. Van D B and Anderson S L 2006 *Energy Fuels* **20** 1886
3. Nakra S, Green R J and Anderson S L 2006 *Combust. Flame* **144** 662
4. Chenoweth K, van Duin A C, Dasgupta S and Goddard III W A 2009 *J. Phys. Chem. A* **113** 1740
5. Davidson D F, Horning D C, Oehlschlaeger M A and Hanson R K 2001 In *Proceedings of the 37th AIAA/ASME/SAE/ASEE Joint Propulsion Conference and Exhibit*, Salt Lake City, UT, July 8-11, 2001, AIAA 01–3707
6. Simonsen J L 1920 *J. Chem. Soc., Trans.* **117** 570
7. Simonsen J L 1922 *J. Chem. Soc., Trans.* **121** 2292
8. Simonsen J L and GopalaRau M 1923 *J. Chem. Soc., Trans.* **123** 549
9. Saei D S S, Khalighi-Sigaroodi F, Pirali-Kheirabadi K, Saei-Dehkordi S S, Alimardani-Naghani F and Fallah A A 2014 *J. Food Safety* **34** 87
10. Salem M Z M, Ali H M and Basalah M O 2014 *BioResources* **9** 7454
11. Kulkarni S G, Bagalkote V S, Patil S S, Kumar U P and Kumar V A 2009 *Propellants Explos. Pyrotech.* **34** 520
12. Sharath N, Reddy K P J, Barhai P K and Arunan E 2015 *Curr. Sci.* **108** 2083
13. Cocker W, Hanna D P and Shannon P V R 1968 *J. Chem. Soc. (C)* 489
14. Feltham E J, Almond M J, Marston G, Ly V P and Wiltshire K S 2005 *Spectrochim. Acta A* **56** 2605
15. Plemenkov V V, Rul S V, Kuzmina L G, Kataeva O N and Litvinov I A 1997 *J. Mol. Struct.* **412** 239
16. Luo D, Pierce J A, Malkina I L and Carter W P 1996 *Int. J. Chem. Kinet.* **28** 1
17. Tkachev A V and Denisov A Y 1991 *Mendeleev Commun.* **1** 98
18. Paulson S E, Orlando J J, Tyndall G S and Calvert J G 1995 *Int. J. Chem. Kinet.* **27** 997
19. Bakhvalov O V, Bagryanskaya I Y, Gatilov Y V, Korchagina D V and Barkhash V A 2002 *Russian J. Org. Chem.* **38** 507
20. Oro J, Han J and Zlatkis A 1967 *Anal. Chem.* **39** 27
21. Badger G M, Donnelly J K and Spotswood T M 1966 *Aust. J. Chem.* **19** 1023
22. Weber K H and Zhang J 2007 *J. Phys. Chem. A* **111** 11487
23. Nagaboopathy M, Vijayanand C, Hegde G, Reddy K P J and Arunan E 2008 *Curr. Sci.* **95** 78
24. Rajakumar B, Reddy K P J and Arunan E 2002 *J. Phys. Chem. A* **106** 8366
25. Rajakumar B, Reddy K P J and Arunan E 2003 *J. Phys. Chem. A* **107** 9782
26. Sharath N, Reddy K P J and Arunan E 2014 *J. Phys. Chem. A* **118** 5927
27. Frisch M J et al. 2009 (Wallingford CT: Gaussian Inc.)
28. CHEMKIN-PRO 15101 2010 (San Diego: Reaction Design)
29. Curtiss L A, Raghavachari K, Redfern P C, Rassolov V and Pople J A 1998 *J. Chem. Phys.* **109** 7764
30. Alexiou A and Williams A 1996 *Combust. Flame* **104** 51
31. Sivaramakrishnan R, Tranter R S and Brezinsky K 2006 *J. Phys. Chem. A* **110** 9388
32. Gudiyella S, Malewicki T, Comandini A and Brezinsky K 2011 *Combust. Flame* **158** 687
33. Wang D, Violi A, Kim D H and Mullholland J A 2006 *J. Phys. Chem. A* **110** 4719
34. Harding L B, Klippenstein S J and Georgievskii Y 2007 *J. Phys. Chem. A* **111** 3789
35. Westmoreland P R, Dean A M, Howard J B and Longwell J P 1989 *J. Phys. Chem.* **93** 8171